$[Me_3SiN(PPh_3)\cdot ICN]$: A New Labile Donor−Acceptor Complex

Rhett Kempe,[†,‡] Elmar Kessenich,[§] and Axel Schulz*[,§]

The Max Planck Institute of Rostock and the Department of Chemistry, Ludwig Maximilians University of Munich, Butenandtstrasse 5-13 (Haus D), D-81377 München, Germany

Received March 9, 2001

The reaction behavior of trimethylsilyl phosphanimine, $Me_3SiNPPh_3$, toward the pseudohalogen species XCN (X = Cl, Br, and I), especially the intermediate formation of $[Me_3SiN(PPh_3)\cdot XCN]$ adduct complexes, was investigated in solution. Only the ICN adduct was shown to be metastable in solution, with respect to further reaction into Ph_3PNCN and Me_3SiX, and can be intercepted. Raman and X-ray data of the ICN adduct revealed a very labile donor−acceptor complex with the iodine atom of the ICN moiety loosely bound to the nitrogen atom of $Me_3SiNPPh_3$. There are two distinct rather long N···I bonds with bond lengths of 2.634(1) and 2.739(14) Å. The structure and bonding are discussed on the basis of natural bond orbital analysis and valence bond considerations.

Introduction

Silylated phosphanimines, Me_3SiNPR_3 (R = Me, Et, Ph), have been frequently used as starting material to introduce the NPR_3 group in reactions with metal and nonmetal halide compounds.[1] Another synthetic route represents the Staudinger reaction in which an azide component is reacted with phosphines (e.g., PR_3).[2] Recently, we have been investigating the reactions of cyanuric azides with PPh_3 resulting, according to the stoichiometry, in mono-, di-, and trisubstituted triphenylphosphanimino-1,3,5-triazines.[3]

The first report on the syntheses of *N*-halogenphosphanimines, Ph_3PNX with X = Cl, Br, I, was published in 1961.[4] The reaction of triphenylphosphanimine with chlorine or bromine yields Ph_3PNX

$$2Ph_3PNH + X_2 \rightarrow Ph_3PNX + [Ph_3PNH_2]X \qquad (1)$$

$$(X = Cl, Br, I)$$

Dehnicke et al. found that in these reactions, side products such as $[Ph_3PNH_2]X_3$, $[Ph_3PNX\cdot X_2]$, $[Ph_3PNH\cdot X_2]$, and $[Ph_3PNPPh_3]X_3$ are formed.[5] A new way to pure Ph_3PNI was introduced in a two-step synthesis by the same group when $Me_3SiNPPh_3$ was reacted with ICl forming a $[Me_3SiNPPh_3\cdot ICl]$ complex. When KF is added, this complex forms Ph_3PNI upon heating (eqs 2 and 3)

$$Me_3SiNPPh_3 + ICl \rightarrow [Me_3SiN(PPh_3)\cdot ICl] \qquad (2)$$

$$[Me_3SiN(PPh_3)\cdot ICl] + KF \rightarrow Me_3SiF + KCl + Ph_3PNI \qquad (3)$$

The acid strength of ICN in solution has been intensively investigated.[6,7] Laurence et al. concluded, on the basis of experimentally determined complex formation enthalpies of ICl, I_2, and ICN adducts, that the order of acid strength depends on the softness (or hardness) of the base. They found an increase of the acid strength along the sequence ICl > I_2 > ICN toward soft bases and ICl > ICN > I_2 toward hard bases.[8]

In this study, we would like to present our results of the reaction of $Me_3SiNPPh_3$ with the pseudohalides XCN (X = Cl, Br, I).

Results and Discussion

Analogous to eq 2, we tried to synthesize the adducts $[Me_3SiN(PPh_3)\cdot XCN]$ with X = Cl, Br, and I. Only for the ICN reaction, we were able to isolate the adduct $[Me_3SiN(PPh_3)\cdot ICN]$ (**1**) in the solid state. The ClCN immediately decomposed $Me_3SiNPPh_3$ to give Me_3SiCl and Ph_3PNCN, while the reaction with BrCN takes longer. Heating or addition of KF resulted in all cases in the immediate formation of Ph_3PNCN. The reaction of $[Me_3SiN(PPh_3)\cdot ICN]$ with KF, especially, represents an easy route to Ph_3PNCN.

Compound **1** has been characterized by Raman spectroscopy and elemental analysis. Single crystals suitable for X-ray diffraction determination were grown from CH_2Cl_2. A view of the molecular structure of **1** is shown in Figure 1. **1** crystallizes in the monoclinic space group *C*2/*c* with 16 molecules in the unit cell. There are two crystallographically different molecules with fairly different bond lengths and angles (Table 1). The view along the *b*-axis of the unit cell is depicted in Figure 2 displaying two different ICN layers. An angle of 106° is found between the two layers. Two-dimensional layerlike molecules are well-known, e.g., in metal halides, chalcogenides, and

* To whom correspondence should be addressed. E-mail: Axel.Schulz@cup.uni-muenchen.de. Fax: +49-89-2180-7492. Tel: +49-89-2180-7763.
† Max Planck Institute of Rostock.
‡ Performed X-ray structure analysis.
§ Ludwig Maximilians University of Munich.

(1) (a) Anfang, S.; Grebe, J.; Möhlen M.; Neumüller, B.; Faza, N.; Massa, W.; Magull, J.; Dehnicke, K. *Z. Anorg. Allg. Chem.* **1999**, *625*, 1395. (b) Heshmatpour, F.; Nusshär, D.; Garbe, R.; Wocadlo, S.; Masa, W.; Dehnicke, K. *Z. Anorg. Allg. Chem.* **1995**, *621*, 443.
(2) Staudinger, H.; Meyer, J. *Helv. Chim. Acta* **1919**, 635.
(3) (a) Kessenich, E.; Klapötke, T. M.; Polborn, K.; Schulz, A. *Eur. J. Inorg. Chem.* **1998**, 2013. (b) Kessenich, K.; Polborn, K.; Schulz, A. *Inorg. Chem.* **2001**, *40*, 1102.
(4) (a) Appelt, R.; Büchler, G. *Z. Anorg. Allg. Chem.* **1961**, *320*, 3. (b) Appelt, R.; Hauss, A. *Z. Anorg. Allg. Chem.* **1961**, *311*, 290.
(5) Grebe, J.; Weller, F.; Dehnicke, K. *Z. Naturforsch.* **1996**, *51b*, 1739.
(6) Bahnick, D. A.; Person, W. B. *J. Chem. Phys.* **1968**, *48*, 5637.
(7) Leeuw, J. de; Zeegers-Huyskens, T. *Spectrochim. Acta* **1976**, *32A*, 617.
(8) Laurence, C.; Queignec-Cabanetos, M., *J. Chem. Soc., Dalton Trans.* **1981**, 2144.

10.1021/ic0102687 CCC: $20.00
Published on Web 08/24/2001

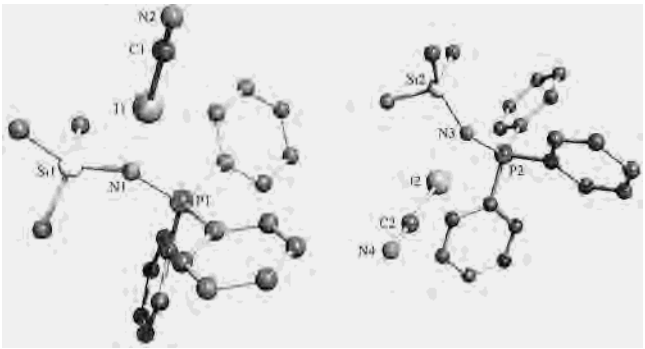

Figure 1. Molecular structure of **1**.

Table 1. Selected Bond Lengths (Å) and Angles (deg) of [$Me_3SiN(PPh_3)$·ICN] (**1**)

N2−C1	1.145(2)	N4−C2	1.163(3)
C1−I1	2.023(1)	I2−C2	2.040(9)
I1−N1	2.634(1)	I2−N3	2.739(14)
N1−Si1	1.734(18)	N3−Si2	1.714(1)
N1−P1	1.569(13)	N3−P2	1.560(9)
N2−C1−I1	176.12(1)	N4−C2−I2	175.92(2)
C1−I1−N1	179.11(1)	C2−I2−N3	177.03(1)
I1−N1−P1	110.74(1)	I2−N3−P2	114.44(2)
I1−N1−Si1	115.87(1)	I2−N3−SI2	109.14(1)
Si1−N1−P1	133.24(2)	Si2−N3−P2	136.38(1)

hydroxides. A superb comprehensive summary on layerlike structures and donor−acceptor interactions is given by Bent.[9]

Structure. The molecular structure of **1** reveals C_1 symmetry in which the nitrogen atom of the PNSi unit is very weakly bound to the ICN molecule. The most characteristic and interesting feature of this type of adducts is their extremely long N···I distance, which is a consequence of the strong "closed-shell interaction" between the ICN and $Me_3SiNPPh_3$ fragments and has received much interest in recent years.[10] This interaction is especially pronounced with soft ligands and generally with larger participating atoms as observed earlier with numerous complexes.[11] The N−I bond is rather long at 2.634(1) and 2.739(14) Å but smaller than the I···N van der Waals interaction (3.70 Å).[12] For comparison, the N−I bond length in the Ph_3PN−I molecule is 2.056 Å.[13] Solid ICN consists of ICN chains with strong attractions between the iodine atom of one ICN molecule and the nitrogen atom of another. An interatomic N···I distance of 2.8 Å was found in solid ICN, which is also far smaller than the sum of the van der Waals radii.[14] The I−CN distance is slightly smaller (2.023 Å) in the adduct than in pure solid ICN (2.03 Å)[15] but substantially longer than the I−CN distance in the isolated gas-phase ICN (1.995 Å).

The environment of the nitrogen atom can be regarded as a slightly distorted trigonal-planar coordination with I−N−P−Si torsion angles of 177.71(81) and 175.30(67)°. The N1−I1−C1 unit is almost linear with an angle of 179.11(1)°. In contrast to isolated ICN, the I1−C1−N2 fragment is slightly bent with an angle of 176.12(1)°.

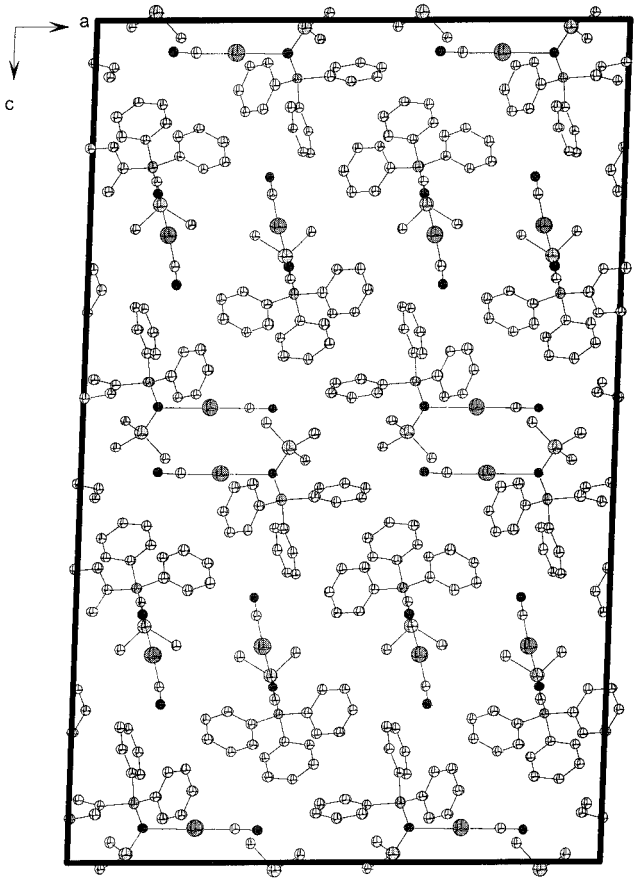

Figure 2. View along the *b*-axis of the unit cell of **1** showing the two different arrangements of the ICN adduct.

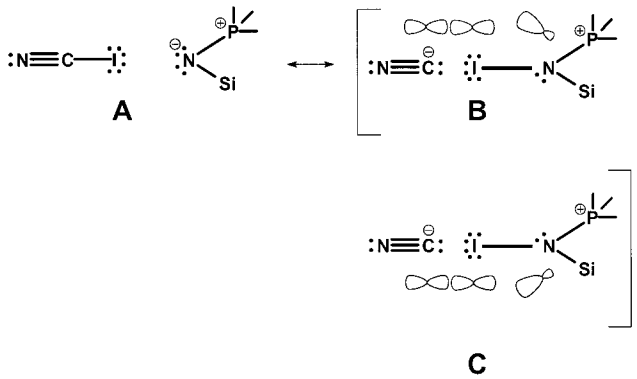

Figure 3. Canonical Lewis structures of **1**.

Bonding. The intriguing structural features of **1** can be rationalized by a qualitative valence bond (VB) consideration. Canonical Lewis structures of types A−C (Figure 3) are easily anticipated. In each of the structures, neither the phosphorus atom nor the iodine atom has expanded its valence shell to use 3d- or 5d-type atomic orbitals (AOs) to form electron-pair bonds. Natural atomic populations of the d-AOs are so small[16] that expanded valence-shell VB structures would be expected to make very minor contributions to the ground-state resonance scheme.[17] The calculated iodine, phosphorus, and nitrogen natural atomic orbital (NAO) net charges are $Q_I = +0.37e$, $Q_P = +2.11e$, and $Q_N = -1.74e$, respectively (Table 2). These partial charges and the calculated covalent bond orders [BO(N−

(9) Bent, H. *Chem. Rev.* **1968**, *68*, 587.
(10) Gramstad, T. *Phosphorus, Sulfur Silicon Relat. Elem.* **1997**, *3*, 241.
(11) Grebe, J.; Geiseler, G.; Harms, K.; Neumüller, B.; Dehnicke, K. *Angew. Chem.* **1999**, *111*, 183; *Angew. Chem. Int. Ed.* **1999**, *38*, 222.
(12) Klapötke, T. M.; Tornieporth-Oetting, I. C. *Nichtmetallchemie*; VCH Verlagsgesellschaft: Weinheim, New York, 1994.
(13) Grebe, J.; Weller, F.; Dehnicke, K. *Z. Naturforsch., B: Chem. Sci.* **1996**, *51*, 1739.
(14) (a) Ketelaar, J. A. A.; Zwartsenberg, J. W. *Recl. Trav. Chim. Pays-Bas* **1939**, *58*, 448. (b) Heiart, R.; Carpenter, G. B. *Acta Crystallogr.* **1956**, *9*, 889.
(15) Abrahams, S. C.; Collin, R. L.; Lipscomb, W. N.; Reed, T. B. *Rev. Sci. Instrum.* **1950**, *21*, 396.
(16) NBO natural population (P: [core]3s(0.83)3p(1.98)3d(0.07); I: [core]-5s(1.93)5p(4.69)5d(0.01).
(17) Harcourt, R. D.; Schulz, A. *J. Phys. Chem. A* **2000**, *104*, 6510.

Table 2. NBO Analysis of **1** and "Naked" ICN (Partial Charges in *e*, Energies in kcal mol^{-1})

	ICN[a]	ICN adduct[b]
partial charges		
N(PNSi)		−1.744
I	0.3588	0.3730
C(ICN)	−0.0290	−0.0300
N(ICN)	−0.3300	−0.4075
charge transfer		
	0.064	
donor−acceptor interaction		
$\sum E^{(2)}$ [NCI → $Me_3SiNPPh_3$]		9.8
$\sum E^{(2)}$ [$Me_3SiNPPh_3$ → ICN]		28.8
total $E^{(2)}$		38.6
$E^{(2)}$ [$sp^{7.10}$-LP(N) → σ^*(IC)][c]		13.05
$E^{(2)}$ [$sp^{14.30}$-LP(N) → σ^*(IC)][c]		9.74
$E^{(2)}$ [p_x-LP(I) → π_x^*(CN)][d]	19.7	18.0
$E^{(2)}$ [p_y-LP(I) → π_y^*(CN)][d]	19.7	19.0

[a] Gas-phase equilibrium structure has been used, see ref 31. [b] X-ray structure has been used. [c] LP = lone pair, both lone pairs on N are mostly composed from p-type atomic orbitals. [d] ICN lies on the *z*-axis.

P) = 0.71, BO(N−I) = 0.05][18] support the conclusion that resonance structure A is the primary structure for **1** with one P−N single bond, one Si−N single bond, and two lone pairs located on the nitrogen atom of the PNSi unit.

Landis and co-workers have developed a valence bond model that works very well in the prediction of molecular shapes for main group molecules.[19] Their prediction is in agreement with our findings. Strong ionic−covalent resonance rationalizes "hypervalent" bonding; such resonances are usually the largest at the linear arrangement, which is nicely in agreement with the experimental finding that the N1−I1−C1 unit is almost linear with an angle of 179.11(1)°.

Investigation of the donor−acceptor interaction between both closed-shell fragments ($Me_3SiNPPh_3$ and ICN) revealed two interactions of the two lone pairs of the nitrogen atom with the empty antibonding σ^* orbital of the I−C bond, corresponding to resonance between structures A ↔ B and A ↔ C, respectively. Hence, the σ bond system of **1** can be referred to as a four-electron, three-center bond (Figure 3). The energy associated with this interaction was estimated by a second-order perturbation approach (10 and 13 kcal mol^{-1}, Table 2), which has been successfully introduced and applied to weak donor−acceptor complexes (such as H-bonded neutral complexes or ion−molecule complexes) by Weinhold et al.[20] These two interactions represent the strongest interactions. However, there is a series of significantly smaller additional interactions with energies between 0.05 and 2 kcal mol^{-1}. Separation of the total interaction between these two fragments ($Me_3SiNPPh_3$ and ICN) shows that mostly the $Me_3SiNPPh_3$ fragment orbitals represent the donor orbitals and the ICN orbitals the acceptor orbitals ($\sum E^{(2)}$ [$Me_3SiNPPh_3$ → ICN] = 28.8 vs 9.8 kcal mol^{-1} for the ICN → $Me_3SiNPPh_3$ interaction, Table 2). The total energy ($\sum E^{(2)}$ [$Me_3SiNPPh_3$ → ICN] + $\sum E^{(2)}$ [ICN → $Me_3SiNPPh_3$]) describing the overall interaction (all donor−acceptor interactions larger than 0.05 kcal mol^{-1}) between these two fragments is 38.6 kcal mol^{-1}.

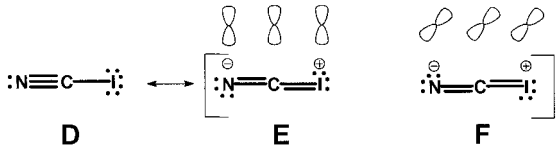

Figure 4. Canonical Lewis structures of ICN describing the π bonds (delocalization of the two iodine p-type lone pairs).

A small charge transfer of 0.064*e* is accompanied with this donor−acceptor interaction. Investigations of the charge distribution of the ICN fragment in comparison with the "isolated" ICN molecule display an interesting feature. Upon adduct formation, a charge redistribution occurs within the ICN fragment with the CN group receiving 0.079*e* and the iodine atom becoming even more positive ($Q_{I,adduct} = +0.373e$ vs $Q_I = +0.359e$ in "isolated" ICN).

The π bonding of the ICN fragment is very similar to that in isolated ICN. There are two interactions of the two p-type lone pairs of the I atom with the π^*(CN) orbitals corresponding to resonance between D ↔ E ↔ F (Figure 4). The estimated energies associated with this type of interaction are 39.4 kcal mol^{-1} ($E^{(2)}$[p_x-LP(I) → π_x^*(CN)] + $E^{(2)}$[p_y-LP(I) → π_y^*(CN)], Table 2) in the free ICN and 37.0 kcal mol^{-1} in the ICN unit of the adduct.

The so-called closed-shell interactions have received a great deal of interest in recent years.[21,22] They comprise of all intermolecular interactions, such as hydrogen bonds, donor−acceptor (Lewis acid−base) or charge-transfer complexes, metallophilic interactions, and any other attractive interactions between atoms and molecules. They are often encountered, especially, with large atoms, so iodine is ideal in this respect. Let it suffice to mention one example which is very similar to **1**: the $L_3P\cdots I_2$ donor−acceptor complexes (e.g., $Ph_3P\cdots I_2$) in which one of the iodines is attached to P with a charge-transfer bond and with a close to linear P···I−I bond angle.[23] In this molecule, the I−I bond length (3.16(2) Å) is considerably longer than that of free iodine and this can be explained by the fact that electron density shifts from the lone electron pair of phosphorus to a σ^* orbital of the iodine molecule.

Raman Spectroscopy. The Raman spectrum was consistent with the presence of pure **1**. Three distinguished normal modes could be assigned to the ICN fragment of adduct **1** in comparison with other experimental data of gaseous and solid ICN, ICN in nonpolar and polar solvents, and other ICN adducts (Table 3). Interestingly, the ICN stretching mode is slightly split (ν_2 = 421/415 cm^{-1}), which is in accord with the two independent ICN molecules in the unit cell. Compared to ICN gas (ν_2 = 485 cm^{-1}, I−C stretch) and ICN in CCl_4 (ν_2 = 487 cm^{-1}), the wavenumbers of the I−C stretches (ν_2) of all adducts and solid ICN appear at lower values. For **1**, this can be best explained by the fact that electron density shifts from the lone pairs of the nitrogen atom (PNSi unit) to the σ^*(I−X) orbital of the ICN molecule. Similar interactions can be discussed for all other adducts. In solid ICN, the interaction of the nitrogen lone pair with the σ^*(I−C) bond of a second unit (ICN: → σ^*(I−CN)) causes this decrease in the wavenumber for ν_2. The

(18) Natural Localized Molecular Orbital bond orders of the NBO analysis: Reed, A. E.; Schleyer, P. v. R. *J. Am. Chem. Soc.* **1990**, *112*, 1434. Reed, A. E.; Schleyer, P. v. R. *Inorg. Chem.* **1988**, *27*, 3969.

(19) (a) Landis, C. R.; Firman, T. K.; Root, D. M.; Cleveland, T. *J. Am. Chem. Soc.* **1998**, *120*, 1842. (b) Landis, C. R.; Cleveland, T.; Firman, T. K. *J. Am. Chem. Soc.* **1998**, *120*, 2641.

(20) (a) Reed, A. E.; Curtiss, L. A.; Weinhold, F. *Chem. Rev.* **1988**, *88*, 899. (b) NBO analysis: The second-order perturbation energy was computed according to $\Delta_{\varphi\varphi^*}E^{(2)} = -2((\langle\varphi|h^F\varphi^*\rangle)^2/(\epsilon_{\varphi^*} - \epsilon_\varphi))$ with h^F being the Fock operator.

(21) Schulz, A.; Aubauer, Ch.; Klapötke, T. M. *THEOCHEM*, in press.

(22) Desiraju, G. *J. Chem. Soc., Dalton Trans.* **2000**, 3745.

(23) Gondfrey, S. M.; Kelly, D. G.; McAuliffe, C. A.; Mackie, A. G.; Pritchard, R. G.; Watson, S. M. *J. Chem. Soc., Chem. Commun.* **1991**, 1163.

Table 3. Vibrational Data of Gaseous ICN, **1**, and Donor−Acceptor Complexes of ICN (wavenumbers in cm^{-1})

	ν_1 C−N stretch	ν_2 I−C stretch	ν_3 ICN bend
ICN_{gas}[a]	2188	485	304
ICN_{solid}	2169	456	329
(CCl_4)·(ICN)[b]	2168	487	319
(pyridine)·(ICN)[b]	2157	429	333
$I(CN)_2^-$[c]	2126	422/425[c]	351/337
1	2147	415/421	325

[a] See ref 32. [b] See ref 7. [c] Symmetrical and antisymmetrical mode, see ref 33.

bending vibration ($\nu_3 = 325\ cm^{-1}$) is relatively unchanged upon complexation. The ν_1 is also little affected by complexation and drops only slightly. Upon complexation, no effect could be observed on the Raman spectrum of the $Me_3SiNPPh_3$ fragment.

Model Adduct Complex [$H_3SiN(PH_3)$·XCN] (X = Cl, Br, I). It is known that for adducts in the solid state and gas phase, structural data can be quite different. Leopold et al. have indicated that the dative or coordinate bond is much shorter in the solid state than in the gas phase, and this change has been associated with the substantial dipole moment of the adduct.[24] It seems that experimental solid-state structural determination is not feasible for the complete range of [$Me_3SiN(PPh_3)$·XCN] complexes, and the only technique for their comprehensive structural study is computations. Moreover, these weakly bound complexes are extraordinarily sensitive to the presence of neighboring molecules. Hence, to obtain a consistent set of data, calculations were carried out on the isolated species. To be able to discuss structural and electronic trends for all three adduct complexes, we have replaced the methyl and phenyl groups with hydrogen atoms [$H_3SiN(PH_3)$·XCN].

Replacing the methyl and phenyl groups with hydrogen atoms has two major effects on the adduct complex: (i) Less electron density is transferred from the PNSi to the XCN unit resulting in a weaker donor−acceptor bond (cf. Tables 2 and 5). (ii) The hybridization on the N atom (PNSi unit) changes; one lone pair represents a p-type atomic orbital whereas the second represents a $sp^{2.42}$ hybrid (ICN adduct). Only the latter one is able to interact with the XCN fragment (Table 5). In [$Me_3SiN(PPh_3)$·ICN], both nitrogen lone pairs possess a small amount of s character ($sp^{7.10}$ and $sp^{14.30}$) and both interact with the XCN fragment leading to stronger donor−acceptor complexes. Apart from these two effects, the observed trends correspond to the following expectation: at the considered level of theory (MP2), the adduct formation of [$H_3SiN(PH_3)$·XCN] (X = Cl, Br, I) represents an exothermic reaction in the gas phase (ΔH_{298}($H_3SiN(PH_3)$·XCN) = −2.04 ClCN, −4.97 BrCN, and −8.38 ICN kcal mol^{-1}) although these adducts are not thermodynamically stable in the gas phase (ΔG_{298}($H_3SiN(PH_3)$·XCN) = 5.70 ClCN, 3.86 BrCN, and 2.72 ICN kcal mol^{-1}). In the solid state, intermolecular interactions play an important role to stabilize these adducts and therefore need to be considered. Chemically similar compounds are stabilized in the solid state, and this stabilization energy lies in the range of 20 ± 5 kcal mol^{-1}.[25] The stability of [$H_3SiN(PH_3)$·XCN] increases from the ClCN toward the ICN complex, which is in accord with the experimental observations for the [$Me_3SiN(PPh_3)$·XCN] system (see Supporting Information).

The increasing stability along the series is also reflected by their bond distances (d(N1−X)), calculated charge transfer, bond orders, and donor−acceptor energies (Tables 4 and 5). The d(N1−X) distance is the largest for [$H_3SiN(PH_3)$·ClCN] with 2.853 Å and the smallest for [$H_3SiN(PH_3)$·ICN] with 2.781 Å. The charge transfer (q_{ct}) and the N1···X bond orders also show a gradual change from [$H_3SiN(PH_3)$·ClCN] toward [$H_3SiN(PH_3)$·ICN]; q_{ct}(Cl) and BO(N1Cl) are the smallest in [$H_3SiN(PH_3)$·ClCN] (0.0097*e* and 0.0064) and the largest in [$H_3SiN(PH_3)$·ICN] (0.0409*e* and 0.0290). Since the electron transfer is associated with the interaction of the nitrogen lone pair (PNSi unit) with the σ^*(X−C) bond (XCN unit), the X−C distance increases in the XCN complexes. This interaction is the largest in the ICN adduct ($E^{(2)}$ [LP(N) → σ^*(X−C)], 4.0 ClCN, 8.2 BrCN, and 14.0 ICN, Table 5), and hence, the largest elongation of the X−C bond is found for the ICN adduct (Δ(d(X−C, adduct) − d(X−C, free XCN)): 0.005 Å ClCN, 0.015 Å BrCN, and 0.034 Å ICN).

The estimated total donor−acceptor energy (see Bonding) is the largest for the ICN, 19.9 kcal mol^{-1}, and decreases toward the ClCN adduct, for which it is only 6.94 kcal mol^{-1} (see Table 5, total $E^{(2)}$).[20] Analogous to the [$Me_3SiN(PPh_3)$·ICN] species, separation of the total interaction between the two fragments (H_3SiNPH_3 and XCN) of [$H_3SiN(PH_3)$·XCN] shows that mostly the orbitals of the PNSi fragment represent the donor orbitals and the XCN orbitals the acceptor orbitals (Table 5).

As expected, the amount of π bonding within the XCN fragment decreases from the ClCN toward the ICN adduct (32.4 and 32.6 kcal mol^{-1} vs 16.7 and 17.0 kcal mol^{-1}).

Experimental Section

General Remarks. Solvents were freshly distilled, dried, and stored under nitrogen. All reactions were carried out under an atmosphere of argon (5.0) in dried glassware. Raman spectra were obtained using a Perkin-Elmer Spectrum 2000R NIR FT. CHN analyses were performed with Analysator Elementar Vario EL. $Ph_3PNSiMe_3$, BrCN, and ICN were prepared according to the procedure given in the literature.[26,27]

Compound 1. A solution of 0.7 g (4.6 mmol) of ICN in CH_2Cl_2 (10 mL) was added to a solution of 1.6 g (4.6 mmol) of $Ph_3PNSiMe_3$ in CH_2Cl_2 (20 mL) at 20 °C in ½ h. The solution was stirred for 2 h. After slow distillation of the solvent, yellow crystals were obtained. $C_{22}H_{24}IN_2PSi$, M = 502.39. Yield: ca. 2.1 g (4.18 mmol, 90%) of pale yellow crystals. Anal. Calcd for $C_{22}H_{24}IN_2PSi$: H, 4.81; C, 52.6; N, 5.58. Found: H, 4.76; C, 51.8; N, 5.65. Raman (200 mW, RT): $\tilde{\nu}$ = 3076 cm^{-1} (4), 3144 (5), 3069 (43), 3061 (61), 3010 (5), 2955 (13), 2893 (20), 2147 (34), 1590 (60), 1574 (12), 1437 (3), 1409 (3), 1185 (10), 1167 (13), 1160 (14), 1113 (6), 1098 (15), 1029 (34), 1000 (100), 930 (2), 858 (4), 752 (3), 713 (5), 685 (5), 666 (6), 619 (16), 604 (18), 598 (16), 538 (10), 421 (66), 415 (55), 384 (80), 325 (1), 275 (8), 254 (22), 225 (14), 206 (15).

Crystal Structure Analysis of 1. $C_{22}H_{24}IN_2PSi$, M = 502.39; crystal size 0.4 × 0.4 × 0.3 mm, light yellow prism, monoclinic, space group $C2/c$, a = 26.991(5) Å, b = 8.338(2) Å, c = 42.892(9) Å, β = 92.05(3)°, V = 9646.7(36) $Å^3$, Z = 16, d_{calcd} = 1.384 Mg/m^3, F(000) = 4032. STOE-IPDS, Mo Kα, λ = 0.710 73 Å, T = 293(2) K, 2θ range = 1.51 to 18.43° in $-24 \le h \le 23$, $-7 \le k \le 7$, $-0 \le l \le 37$.

(24) (a) Fiacco, D. L.; Mo, Y.; Hunt, S. W.; Ott, M. E.; Roberts, A.; Leopold, K. R. *J. Phys. Chem. A* **2001**, *105*, 484. (b) Fiacco, D. L.; Torro, A.; Leopold, K. R. *Inorg. Chem.* **2000**, *39*, 37. (c) Fiacco, D. L.; Hunt, S. W. Leopold, K. R. *J. Phys. Chem. A* **2000**, *104*, 8323. (d) Burns, W. A.; Phillips, J. A.; Canagaratna, M.; Goodfriend, H.; Leopold, K. R. *J. Phys. Chem. A* **1999**, *103*, 7445. (e) Canagaratna, M.; Phillips, J. A.; Goodfriend, H.; Leopold, K. R. *J. Am. Chem. Soc.* **1996**, *118*, 5290. (f) Leopold, K. R.; Canagaratna, M.; Phillips, J. A. In *Advances in Molecular Structure Research*; Hargittai, M., Hargittai, I., Eds.; JAI Press: Greenwich, CT, 1996; Vol. 2, p 103.

(25) Rossini, F. D.; Wagman, D. D.; Evans, W. H.; Levine, S.; Jaffe, I. *Selected Values of Chemical Thermodynamic Properties*; United States Government Printing Office: Washington, DC, 1952.

(26) Birkhofer, L.; Ritter, A.; Richter, P. *Chem. Ber.* **1963**, *96*, 2750.

(27) Brauer, G. *Handbuch der präparativen anorganischen Chemie*, 3rd ed.; Ferdinand Enke Verlag: Stuttgart, 1978; pp 632−633.

Table 4. Calculated Structural Data (MP2) of XCN and the Model Adduct Complexes [$H_3SiN(PH_3)$·XCN] (Bond lengths (Å) and Angles (deg))[a]

	ClCN	ClCN adduct	BrCN	BrCN adduct	ICN	ICN adduct	H_3SiNPH_3
d(N1−X)		2.853		2.789		2.781	
d(C−X)	1.654	1.659	1.798	1.813	2.017	2.051	
d(C−N2)	1.186	1.186	1.187	1.187	1.188	1.188	
d(N1−P)		1.560		1.564		1.572	1.546
d(N1−Si)		1.720		1.726		1.735	1.705
∠(X−C−N2)		179.8		179.7		179.7	
∠(Si−N1−P)		134.3		132.5		129.3	142.0
∠(C−X−N1)		177.4		177.2		177.3	
∠(X−N1−P−Si)		180.0		179.9		180.0	

[a] N1, N atom of the H_3SiNPH_3 fragment; N2, N atom of the XCN fragment.

Table 5. NBO Analysis of the Model Adduct Complexes [$H_3SiN(PH_3)$·XCN] and the Isolated XCN Molecules (Partial Charges in *e*, Energies in kcal mol^{-1})[a]

	ClCN	ClCN adduct	BrCN	BrCN adduct	ICN	ICN adduct	H_3SiNPH_3
				partial charges			
X	0.1281	0.1478	0.2338	0.2509	0.3601	0.3744	
C(XCN)	0.2190	0.2179	0.1009	0.0972	−0.0285	−0.0367	
N(XCN)	−0.3471	−0.3755	−0.3347	−0.37031	−0.3316	−0.3785	
N(PNSi)		−1.6627		−1.6675		−1.6722	−1.6544
P		1.3353		1.3303		1.3222	1.3534
Si		1.3399		1.3356		1.3290	
				charge transfer			
		0.0097		0.0222		0.0409	
				donor−acceptor interaction			
$\sum E^{(2)}$ [NCX → $Me_3SiNPPh_3$]		2.27		2.98		3.4	
$\sum E^{(2)}$ [$Me_3SiNPPh_3$ → XCN]		4.67		9.23		16.5	
total $E^{(2)}$		6.94		12.2		19.9	
$E^{(2)}$ [LP(N) → σ^*(XC)][b]		4.0		8.2		14.0	
N1−X NLMO bond order		0.0064		0.0144		0.0290	
$E^{(2)}$ [p_x-LP(X) → π_x^*(CN)][c]	32.0	32.4	26.3	25.5	18.6	16.7	
$E^{(2)}$ [p_y-LP(X) → π_y^*(CN)][c]	32.0	32.6	26.3	25.7	18.8	17.0	

[a] MP2-optimized geometries. [b] LP = lone pair, one lone pair in [$H_3SiN(PH_3)$·XCN] is a pure p-AO whereas the other is almost an sp^2 hybrid. Only the latter one is able to interact with the σ^*(X−C) orbital. In contrast to [$H_3SiN(PH_3)$·XCN], the situation in [$Me_3SiN(PPh_3)$·XCN] is slightly different since both lone pairs are almost pure p-type AOs with only a small amount of s character. Both lone pairs interact with the σ^*(X−C) orbital (see Table 2). [c] ICN lies on the *z*-axis.

Reflections collected, 6237; independent reflections, 3435 (R_{int} = 0.0313); observed reflections, 2732 ($I > 2\sigma(I)$). Structure solution program was the SHELXS-86 (Sheldrick G. M. University of Göttingen: Germany, 1986), direct methods, final *R* indices [$I > 2\sigma(I)$]: R1 = 0.0396, wR2 = 0.0982, R1 = 0.0528, wR2 = 0.1047 (all data), GOF on F^2 = 1.036, 437 refined parameters, program used was SHELXL-93 (Sheldrick G. M. University of Göttingen: Germany, 1993).

Computational Methods

Computations have been carried out using the G98 program suite.[28] A 6-31G(d,p) standard basis set was applied for all atoms, except for the halogens for which multielectron-adjusted quasirelativistic effective core potentials with the electronic configuration of Cl [Ne], Br [Ar]d^{10}, and I [Kr]d^{10} were used. For the halogens, a (5s5p1d)/(3s3p1d) valence basis set (311,311,1) was used. Both the pseudopotentials and the corresponding basis sets were those of the Stuttgart group.[29]

Model Compounds [$H_3SiN(PH_3)$·XCN] (X = Cl, Br, and I). Full geometry optimizations were carried out at the MP2 level and all stationary points were characterized by a frequency analysis. Natural bond orbital (NBO) analyses[20,30] were carried out to investigate the bonding in all molecules at the HF level utilizing the optimized MP2 geometry. The computed geometrical parameters for all molecules are collected in Table 4 and selected results of the NBO analyses in Table 5. The computed frequencies, relative energies, and absolute energies are given as Supporting Information.

(28) Frisch, M. J.; Trucks, G. W.; Schlegel, H. B.; Scuseria, G. E.; Robb, M. A.; Cheeseman, J. R.; Zakrzewski, V. G.; Montgomery, J. A., Jr.; Stratmann, R. E.; Burant, J. C.; Dapprich, S.; Millam, J. M.; Daniels, A. D.; Kudin, K. N.; Strain, M. C.; Farkas, O.; Tomasi, J.; Barone, V.; Cossi, M.; Cammi, R.; Mennucci, B.; Pomelli, C.; Adamo, C.; Clifford, S.; Ochterski, J.; Petersson, G. A.; Ayala, P. Y.; Cui, Q.; Morokuma, K.; Malick, D. K.; Rabuck, A. D.; Raghavachari, K.; Foresman, J. B.; Cioslowski, J.; Ortiz, J. V.; Stefanov, B. B.; Liu, G.; Liashenko, A.; Piskorz, P.; Komaromi, I.; Gomperts, R.; Martin, R. L.; Fox, D. J.; Keith, T.; Al-Laham, M. A.; Peng, C. Y.; Nanayakkara, A.; Gonzalez, C.; Challacombe, M.; Gill, P. M. W.; Johnson, B.; Chen, W.; Wong, M. W.; Andres, J. L.; Head-Gordon, M.; Replogle, E. S.; Pople, J. A. *Gaussian 98*, revision A.6; Gaussian, Inc.: Pittsburgh, PA, 1998.

(29) Andrae, D.; Häussermann, U.; Dolg, M.; Stoll, H.; Preuss, H. *Theor. Chim. Acta* **1990**, *77*, 123.

(30) (a) NBO Version 3.1: Glendening, E. D.; Reed, A. E.; Carpenter, J. E.; Weinhold, F. (b) Carpenter, J. E.; Weinhold, F. *J. Mol. Struct. (THEOCHEM)* **1988**, *169*, 41. (c) Foster, J. P.; Weinhold, F. *J. Am. Chem. Soc.* **1980**, *102*, 7211. (d) Reed, A. E.; Weinhold, F. *J. Chem. Phys.* **1983**, *78*, 4066. (e) Reed, A. E.; Weinstock, R. B.; Weinhold, F. *J. Chem. Phys.* **1985**, *83*, 735. (f) Reed, A. E.; Schleyer, P. v. R. *J. Am. Chem. Soc.* **1987**, *109*, 7362. (g) Reed, A. E.; Schleyer, P. v. R. *Inorg. Chem.* **1988**, *27*, 3969. (h) Weinhold, F.; Carpenter, J. E. *The Structure of Small Molecules and Ions*; Plenum Press: New York, 1988; p 227.

(31) Cazzoli, G.; Esposti, C. D.; Favero, P. G. *J. Mol. Struct.* **1978**, *48*, 1.

(32) Nakamoto, K. *Infrared and Raman Spectra of Inorganic and Coordination Compounds*, Part A, 5th ed.; Wiley & Sons: New York, **1997**; p 178.

(33) Tebbe, K. F.; Fröhlich, R. *Z. Anorg. Allg. Chem.* **1983**, *505*, 7.

NBO population analysis for [$Me_3SiN(PPh_3)$·ICN] was carried out with the structure fixed at that determined from X-ray analysis of **1** to investigate the bonding and hybridization in this experimentally observed species [single point at HF level].

Acknowledgment. A.S. thanks Prof. Dr. T. M. Klapötke (LMU München) for his generous support. Financial support from the LMU München is gratefully acknowledged. We thank the Leibniz Rechenzentrum (München) for a generous allocation of CPU time.

Supporting Information Available: Crystallographic data in cif format for compound **1** and total energies and calculated wavenumbers of all [$H_3SiN(PH_3)$·XCN; X = Cl, Br, and I] species. This material is available free of charge via the Internet at http://pubs.acs.org. Crystallographic data (excluding structure factors) for the structure reported in this paper have been deposited with the Cambridge Crystallographic Data Centre as supplementary publication no. CCDC-164521. Copies of the data can be obtained free of charge on application to CCDC, 12 Union Road, Cambridge CB2 1EZ, UK (fax: (+44) 1223−336−033; e-mail: deposit@ccdc.cam.ac.uk).

IC0102687